JOC*Article*

Computational Study on the 1,2-Rearrangement in β-(Nitroxy)vinyl and β-(Acetoxy)vinyl Radicals

Uta Wille*

ARC Centre of Excellence in Free Radical Chemistry and Biochemistry, The University of Melbourne, VIC 3010, Australia, and BIO21 Molecular Science and Biotechnology Institute, The University of Melbourne, 30 Flemington Road, VIC 3010, Australia

uwille@unimelb.edu.au

Received September 30, 2005

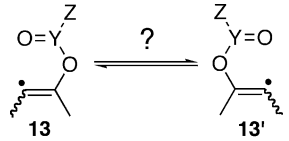

The 1,2-nitroxyl and 1,2-acetoxyl rearrangement in β-(nitroxy)vinyl and β-(acetoxy)vinyl radicals **13a** and **13b**, respectively, has been studied for the gas phase with various ab initio and density functional methods. The energetically most favorable pathway for **13a** is calculated to proceed via reversible fragmentation/radical addition through transition state **I-19a**. In the case of **13b**, rearrangement through a five-membered ring transition state **III-16b** and the fragmentation/radical addition pathway via transition state **I-19b** are competing processes. Mulliken and natural population analysis reveal a certain degree of charge separation in **III-16a/b** that may indicate a potential solvent effect on the rearrangement rate. A stepwise group migration through a cyclic radical intermediate **V-18a/b** or rearrangement through a three-membered ring transition state **II-15a/b** can be ruled out for both vinyl radicals. A comparison of the results of the calculations with experimental findings provides important insights into the kinetics of "self-terminating radical oxygenations". A significant method dependence on the outcome of the calculations was observed, which revealed the unsuitability of the UHF, MP2, B3LYP, and mPW1PW91 methods for computing these radical rearrangement processes. The results from BHandHLYP/cc-pVDZ calculations showed the best agreement with single-point energy calculations performed at the QCISD and CCSD(T) levels of theory.

Introduction

β-(Nitroxy)vinyl and β-(acyloxy)vinyl radicals are formed by attack of nitrate radicals ($NO_3^•$) or acyloxyl radicals [RC(O)O•], respectively, at C≡C triple bonds. This radical addition is the initial step in "self-terminating radical oxygenations", a recently discovered concept in synthetic radical chemistry.[1] Scheme 1 illustrates an exemplary reaction sequence and the proposed mechanism.

Addition of O-centered radicals XO• to 5-cyclodecynone (**1**) leads to the isomeric vinyl radicals **2** and **3** that undergo transannular cyclization onto the carbonyl group. The resulting allyloxyl radicals **5** and **6** subsequently attack the C=C double bond in a 3-exo fashion to give the α-oxy radical intermediates **8** and **9** that decompose into the isomeric α,β-epoxy ketones **11** and **12** through homolytic cleavage of the O−X bond under release of a radical X•.[2−6]

When this reaction was performed with $NO_3^•$, **11** and **12** were exclusively formed.[2a] With other inorganic radicals, for example, the hydroxyl (HO•) or the sulfate radical anion ($SO_4^{•-}$), however, and with organic O-centered radicals, for example, acyloxyl [RC(O)O•] or alkoxyacyloxyl radicals [ROC(O)O•], a third product, identified as the spirodiketone **10**, was obtained. Compound **10** is presumably formed through β-cleavage in **5**,

(1) Dreessen, T.; Jargstorff, C.; Lietzau, L.; Plath, C.; Stademann, A.; Wille, U. *Molecules* **2004**, *9*, 480.

(2) XO• = $NO_3^•$: (a) Wille, U.; Plath, C. *Liebigs Ann./Recl.* **1997**, 111. (b) Wille, U.; Lietzau, L. *Tetrahedron* **1999**, *55*, 10119. (c) Lietzau, L.; Wille, U. *Heterocycles* **2001**, *55*, 377. (d) Wille, U. *Chem.—Eur. J.* **2002**, *8*, 340. (e) Stademann, A.; Wille, U. *Aust. J. Chem.* **2004**, *57*, 1055.

(3) XO• = $SO_4^{•-}$: Wille, U. *Org. Lett.* **2000**, *2*, *3485*.

(4) XO• = HO•: Wille, U. *Tetrahedron Lett.* **2002**, *43*, 1239.

(5) XO• = RC(O)O•: Wille, U. *J. Am. Chem. Soc*. **2002**, *124*, 14.

(6) XO• = ROC(O)O•, ROC(O)C(O)O•, $R_2NC(O)O^•$, $R_2NO^•$, RO•: (a) Jargstorff, C.; Wille, U. *Eur. J. Org. Chem*. **2003**, 2173. (b) Sigmund, D.; Schiesser, C. H.; Wille, U. *Synthesis* **2005**, 1437.

10.1021/jo0520543 CCC: $33.50
Published on Web 04/29/2006

SCHEME 1

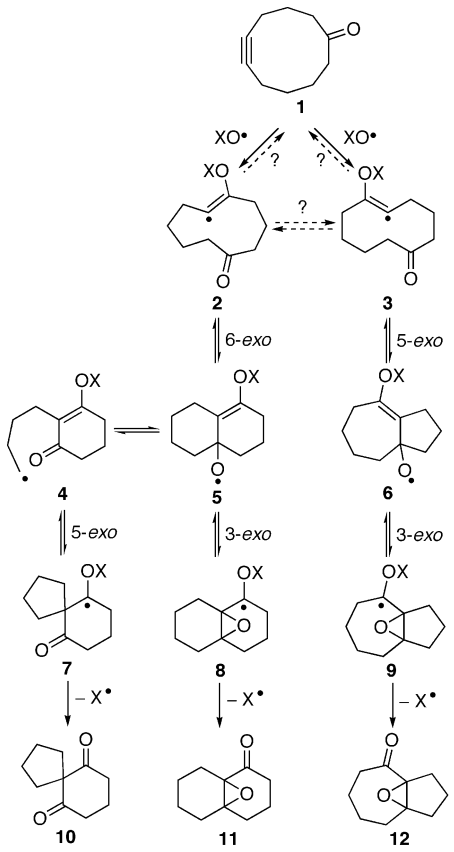

XO•	total yield / %	ratio 10:11:12
NO_3•	77	0:57:43
SO_4•⁻	50	14:43:43
HO•	82	82:12:6
4-$MeC_6H_4C(O)O$•	93	90:5:5
4-$FC_6H_4C(O)O$•	88	84:9:7
MeOC(O)O•	84	79:12:9

followed by 5-exo cyclization in **4** and a terminating homolytic fragmentation in **7**.[7] Our finding that the yield of **10** was regularly significantly higher than 50%, the value that would be expected as a maximum because the initial radical attack should occur with the same probability at either site of the sterically unhindered C≡C bond in **1**, could only be explained if the initial radical addition is reversible and if vinyl radical **3** could directly rearrange into **2** (and vice versa).

Whereas rearrangements in the corresponding *β*-(nitroxy)-alkyl and *β*-(acyloxy)alkyl radicals have been extensively examined by both computational and experimental methods in recent years,[8] similar group migrations in vinyl radicals were not studied so far by either method.[9] To get a deeper

SCHEME 2

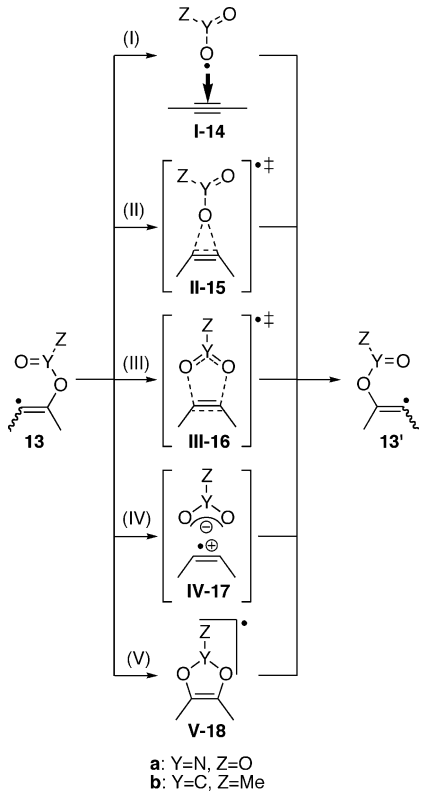

understanding of the mechanism proposed in Scheme 1, ab initio and density functional theory (DFT) calculations were performed on rearrangements in vinyl radicals **13a** and **13b** (Scheme 2), which served as simplified models for the nitroxyvinyl and acyloxyvinyl radicals **2** and **3** [with X = NO_2 or MeC(O), respectively].

Scheme 2 shows the potential mechanistic pathways for the migrations in question: (I) reversible fragmentation/radical addition via an intermediate radical−alkyne association complex **I-14**, (II) concerted [1,2] rearrangement through a cyclic three-membered transition state **II-15**, (III) concerted [3,2] rearrangement through a cyclic five-membered transition state **III-16**, (IV) formation of a contact ion pair **IV-17** that collapses to the product radical, and (V) reaction through a cyclization, a ring-opening sequence involving a five-membered ring intermediate **V-18**.

Theoretical Methods

The calculations were carried out using the Gaussian 03 program.[10] Geometry optimizations were performed using standard gradient techniques at the UHF/6-311G**, MP2/6-311G**,

(7) Formation of **10** from radical intermediate **6** through a fragmentation/cyclization sequence similar to that of **5** is kinetically very unlikely. For details, see: Wille, U.; Jargstorff, C. *J. Chem. Soc., Perkin Trans. 1* **2002**, 1036.

(8) (a) Beckwith, A. L. J.; Crich, D.; Duggan, P. J.; Yao, Q. *Chem. Rev.* **1997**, *97*, 3273. (b) Zipse, H.; Bootz, M. *J. Chem. Soc., Perkin Trans. 2* **2001**, 1566. (c) Choi, S.-Y., Crich, D.; Horner, J. H.; Huang, X.; Newcomb, M.; Whitted, P. O. *Tetrahedron* **1999**, *55*, 3317. (d) Zipse, H. *J. Am. Chem. Soc*. **1997**, *119*, 1087. (e) Crich, D.; Filzen, G. F. *J. Org. Chem.* **1995**, *60*, 4834. (f) Zipse, H. *J. Chem. Soc., Perkin Trans. 2* **1996**, 1797.

(9) Isotopic-labeling experiments have shown that *o*-(acyloxy)aryl radicals do not undergo an ester shift because of the inability of the aryl radical to achieve suitable orbital overlap: (a) Evanochenko, W. T.; Shevlin, P. *J. Org. Chem.* **1979**, *44*, 4426. (b) Shahidi, F.; Tidwell, T. T. *Can. J. Chem.* **1982**, *60*, 1092.

(10) Frisch, M. J.; Trucks, G. W.; Schlegel, H. B.; Scuseria, G. E.; Robb, M. A.; Cheeseman, J. R.; Montgomery, J. A., Jr.; Vreven, T.; Kudin, K. N.; Burant, J. C.; Millam, J. M.; Iyengar, S. S.; Tomasi, J.; Barone, V.; Mennucci, B.; Cossi, M.; Scalmani, G.; Rega, N.; Petersson, G. A.; Nakatsuji, H.; Hada, M.; Ehara, M.; Toyota, K.; Fukuda, R.; Hasegawa, J.; Ishida, M.; Nakajima, T.; Honda, Y.; Kitao, O.; Nakai, H.; Klene, M.; Li, X.; Knox, J. E.; Hratchian, H. P.; Cross, J. B.; Bakken, V.; Adamo, C.; Jaramillo, J.; Gomperts, R.; Stratmann, R. E.; Yazyev, O.; Austin, A. J.; Cammi, R.; Pomelli, C.; Ochterski, J. W.; Ayala, P. Y.; Morokuma, K.; Voth, G. A.; Salvador, P.; Dannenberg, J. J.; Zakrzewski, V. G.; Dapprich, S.; Daniels, A. D.; Strain, M. C.; Farkas, O.; Malick, D. K.; Rabuck, A. D.; Raghavachari, K.; Foresman, J. B.; Ortiz, J. V.; Cui, Q.; Baboul, A. G.; Clifford, S.; Cioslowski, J.; Stefanov, B. B.; Liu, G.; Liashenko, A.; Piskorz, P.; Komaromi, I.; Martin, R. L.; Fox, D. J.; Keith, T.; Al-Laham, M. A.; Peng, C. Y.; Nanayakkara, A.; Challacombe, M.; Gill, P. M. W.; Johnson, B.; Chen, W.; Wong, M. W.; Gonzalez, C.; Pople, J. A. *Gaussian 03*, revision B.04, Gaussian, Inc.: Pittsburgh, PA, 2004.

TABLE 1. Relative Energies Δ*E* (in kJ mol^{-1}) for Stationary Points in the Nitroxyl Shift of 2-(Nitroxy)-2-butenyl Radical (13a)[a]

	***E*-13a**	***Z*-13a**	***E*-13$_{pl}$a**	**I-14a**	**III-16a**	**V-18a**	**I-19a**	**V-20a**	**21a**
UHF/	0.0	−3.4	14.4	53.6[b]	148.9	−94.8	115.1	89.2	[c]
6-311G**		*−3.2*	*12.8*	*46.1*	*144.1*	*−89.5*	*103.3*	*83.3*	
B3LYP/	0.0	−5.0	[d]	38.9	75.6	[d]	51.9	54.8	[d]
6-311G**		*−4.8*		*31.2*	*71.2*		*46.2*	*51.2*	
mPW1PW91/	0.0	−4.3	[d]	65.5	89.8	[d]	70.7	58.1	−70.3
6-311G**		*−4.1*		*57.3*	*85.1*		*64.0*	*54.4*	*−75.1*
mPW1K/	0.0	−3.0	[d]	92.4	104.7	−131.7	92.5	62.9	−124.6
6-31+G**		*−2.9*		*84.2*	*99.4*	*−128.2*	*84.2*	*59.0*	*−128.0*
BHandHLYP/	0.0	−4.1	[d]	74.1	100.9	−121.5	78.1	72.4	−114.2
6-311G**		*−3.9*		*66.4*	*95.5*	*−118.2*	*70.5*	*68.0*	*−118.0*
BHandHLYP/	0.0	−4.3		83.3	105.8	−123.3	86.2	71.4	−117.0
cc-pVDZ		*−4.0*		*75.4*	*100.5*	*−120.4*	*78.4*	*67.0*	*−120.9*
BHandHLYP/	0.0	−3.1		76.0	102.1	−125.4	80.3	71.8	−115.8
cc-pVTZ		*−3.0*		*67.7*	*96.8*	*−121.7*	*72.5*	*67.5*	*−119.6*
BHandHLYP/	0.0	−2.5		75.9	99.3	−127.6	78.9	69.8	−117.5
aug-cc-pVTZ		*−2.5*		*67.6*	*93.9*	*−123.6*	*70.9*	*65.6*	*−121.1*
ROMP2/ 6-311G**[e]	0.0	−4.8		102.8	116.7	−102.9	105.0	71.0	−115.7
ROMP2/ 6-311G**[f]	0.0	−4.6		102.2	116.4	−102.9	90.0	69.9	−117.1
ROMP2/ cc-pVDZ[f]	0.0	−4.7		106.5	116.0	−102.4	94.8	68.2	−120.3
QCISD/ cc-pVDZ[f]	0.0	−4.7		81.7	113.9	−112.3	93.9	75.4	−121.0
CCSD(T)/ cc-pVDZ[f]	0.0	−4.9		85.3	108.8	−110.1	91.0	71.5	−129.7
CCSD(T)/ cc-pVTZ[f]	0.0	−3.6		82.8	100.5	−124.6	86.3	66.1	−137.3

[a] Data in italics include the zero-point vibrational energy correction (ZPE). [b] Different geometry; see text. [c] Fragmention proceeds via two sequential bond cleavages; see ref 19. [d] Structure could not be located. [e] Single-point calculation on BHandHLYP/6-311G** optimized geometry. [f] Single-point calculation on BHandHLYP/aug-cc-pVTZ optimized geometry.

B3LYP/6-311G**, mPW1PW91/6-311G**, mPW1K/6-31+G**,[11] BHandHLYP/6-311G**, BHandHLYP/cc-pVDZ, BHandHLYP/cc-pVTZ, and BHandHLYP/aug-cc-pVTZ levels of theory. All ground and transition states were verified by vibrational frequency analysis. For selected geometries, further single-point ROMP2 (restricted open-shell Møller−Plesset pertubation theory truncated at the second order),[12] QCISD, and CCSD(T) calculations were performed using the cc-pVDZ and the cc-pVTZ basis set on the BHandHLYP/6-311G** and BHandHLYP/aug-cc-pVTZ optimized structures. The charge distribution has been characterized through Mulliken as well as natural population analysis (NPA), as implemented in Gaussian 03. Spin densities were taken from the BHandHLYP/aug-cc-pVTZ calculations. The spin expectation value, $\langle s^2 \rangle$, was very close to 0.75 in all DFT calculations after spin annihilation. In some UHF transition state geometry optimizations and QCISD and CCSD(T) single-point calculations, however, the $\langle s^2 \rangle$ value was significant [for example, in **20a**: 0.9607 (UHF) and 0.8814 (QCISD and CCSD(T)) after spin annihilation]. To assess the quality of the wave function, T_1 diagnostics were exemplarily performed for the rearrangement of **13a**. They revealed a T_1 value of 0.039 for **20a**, 0.030 for **21a**, and ≈ 0.023 for all other geometries. The Gaussian output files for all structures in this study are available as electronic Supporting Information.

Results and Discussion

Rearrangement of the β-(Nitroxy)vinyl Radical 13a: The stationary points identified in the rearrangement of the β-(nitroxy)vinyl radical **13a** are shown in Figure 1, together with the imaginary frequencies associated with the reaction coordinate of the various transition states and spin densities for key structures.

At all levels of theory, two geometrical isomers with *E* and *Z* configurations at the C=C double bond were found for **13a**, which both show the nitrate group twisted out of the plane of the carbon framework by about 106°. Only the UHF/6-311G** calculations revealed also a planar conformation, ***E*-13$_{pl}$a**, which is, however, higher in energy by about 14 kJ mol^{-1} compared to that of ***E*-13a**. Independent of the method, ***Z*-13a** is slightly more stable by up to 5.0 kJ mol^{-1} than ***E*-13a**. Because *E*/*Z* isomerization in vinyl radicals proceeds with very low activation barriers,[13] **13a** should exist in an equilibrium mixture of ***E*-13a** and ***Z*-13a**. Table 1 compiles the energies of all stationary points in the rearrangement process relative to ***E*-13a**.

An examination of the data reveals a significant method-dependent outcome. Besides the above-mentioned finding that the planar vinyl radical ***E*-13$_{pl}$a** could not be located with DFT methods, UHF also calculates a different and slightly less-stable geometry for the $NO_3^{\bullet}$−2-butyne association complex **I-14a**, in which the nitrate moiety is located in about a 3.5 Å distance like a propeller above the alkyne (not shown).[14] In addition, UHF failed to locate transition state **21a** (see later). The latter structure was also not located at the B3LYP/6-311G** level of theory, and both B3LYP and mPW1PW91 were unable to find the cyclic radical intermediate **V-18a**.[15] MP2/6-311G** calculations could only locate the vinyl radicals ***E*/*Z*-13a** and transition state **V-20a** (data not shown). On the other hand, all rele-

(11) (a) Lynch, B. J.; Fast, P. L.; Harris, M.; Truhlar, D. G. *J. Phys. Chem. A* **2000**, *104*, 4811. (b) Zhao, Y.; Pu, J.; Lynch, B. J.; Truhlar, D. G. *Phys. Chem. Chem. Phys.* **2004**, *6*, 673. (c) Lynch, B. J.; Truhlar, D. G. *J. Phys. Chem. A* **2002**, *106*, 842.

(12) (a) Møller, C.; Plesset, M. S. *Phys. Rev.* **1934**, *46*, 618. (b) Head-Gordon, M.; Pople, J. A.; Frisch, M. J. *Chem. Phys. Lett.* **1988**, *153*, 503. (c) Madebene, B.; Solimannejad, M.; Alikhani, M. E. *THEOCHEM* **2004**, *673*, 239.

(13) Curran, D. P.; Porter, N. A.; Giese, B. *Stereoselectivity of Radical Reactions*; VCH: Weinheim, New York, Basel, Cambridge, Tokyo, 1996.

(14) This geometry was also located with the BHandHLYP method and found to be higher in energy by up to 5 kJ mol^{-1}.

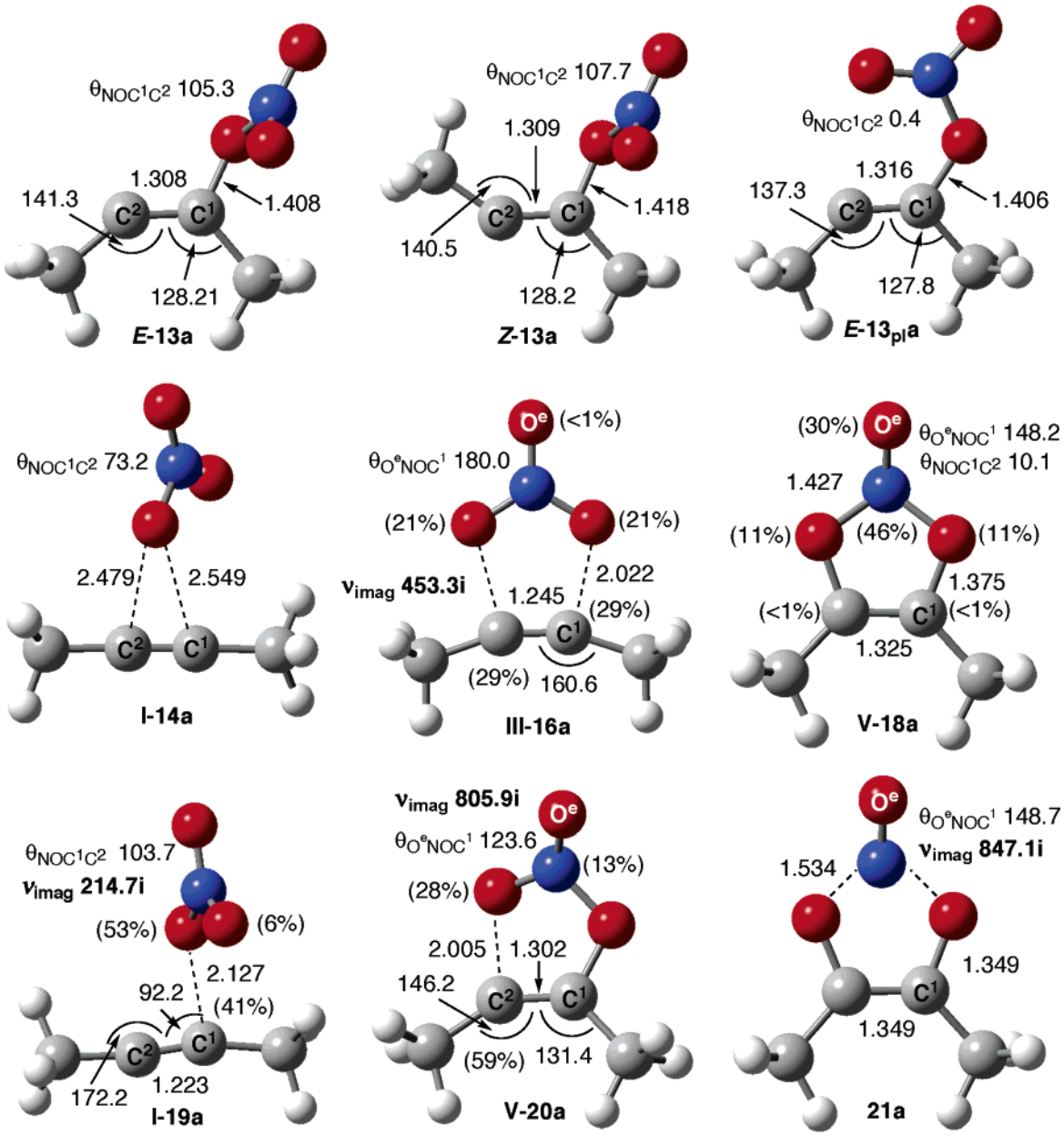

FIGURE 1. Geometrical parameters (bond lengths in Å; angles and dihedral angles, θ, in degrees) of ground and transition states (imaginary frequencies, ν_{imag}, in cm^{-1}) and spin density distributions (in percent, in brackets) for some key structures in the rearrangement of 2-(nitroxy)-2-butenyl radical **13a** (***E*-13$_{pl}$a**, UHF/6-311G**; all other geometries, BHandHLYP/cc-pVDZ; spin densities, BHandHLYP/aug-cc-pVTZ).

vant ground and transition states could be located with the BHandHLYP method. No significant basis set dependency was observed; however, the large cc-pVTZ and aug-cc-pVTZ basis sets lead to generally slightly lower energies than cc-pVDZ and are comparable with the results from the BHandHLYP/6-311G** computations. The not entirely convincing outcome of the mPW1K calculations (e.g., underestimation of transition states **III-16a** and **V-20a**, overestimation of ground states **I-14a** and **V-18a**) may be due to the fact that the mPW1K/6-31+G** method was optimized for hydrogen abstractions and not for radical additions to π systems.[11] In contrast to this, the B3LYP and mPW1PW91 computed energies are significantly too low,[15] whereas especially the energies for the transition states **III-16a**, **I-19a**, and **V-20a** derived from UHF calculations are too high. The MP2/6-311G** calculations revealed an enormous activation energy of some 155 kJ mol^{-1} to reach transition state **V-20a**. All these findings lead to the conclusion that UHF, MP2, B3LYP, and mPW1PW91 are clearly not suitable for the study of this radical rearrangement.[16] No clear conclusion can be

(15) Hybrid density functionals with a low Hartree−Fock exchange (20% in B3LYP and 25% in mPW1PW91) are known to frequently underestimate activation barriers in radical reactions, which results in not very well-contoured potential surfaces; see, for example: Schiesser, C. H.; Matsubara, H.; Ritsner, I.; Wille, U. *Chem. Commun.* **2006**, 1067. Energetically, intermediate **V-18a** sits in a deep well with regard to the reverse ring opening, but only in a very shallow well with regard to its unimolecular decomposition through transition state **21a** (see text). Both the B3LYP and the mPW1PW91 calculations "missed" the energy minimum in which **V-18a** is located and could only identify a van der Waals complex of the diketone **22** and nitrogen oxide.

(16) This supports the finding by others that MP2 is too erratic for the general use with radicals; see: Henry, D. J.; Parkinson, C. J.; Radom, L. *J. Phys. Chem. A* **2002**, *106*, 7927 and references therein.

SCHEME 3. Potential Energy Surface of the Rearrangement of Radical 13a (BHandHLYP/cc-pVDZ Level of Theory, ZPE Included)

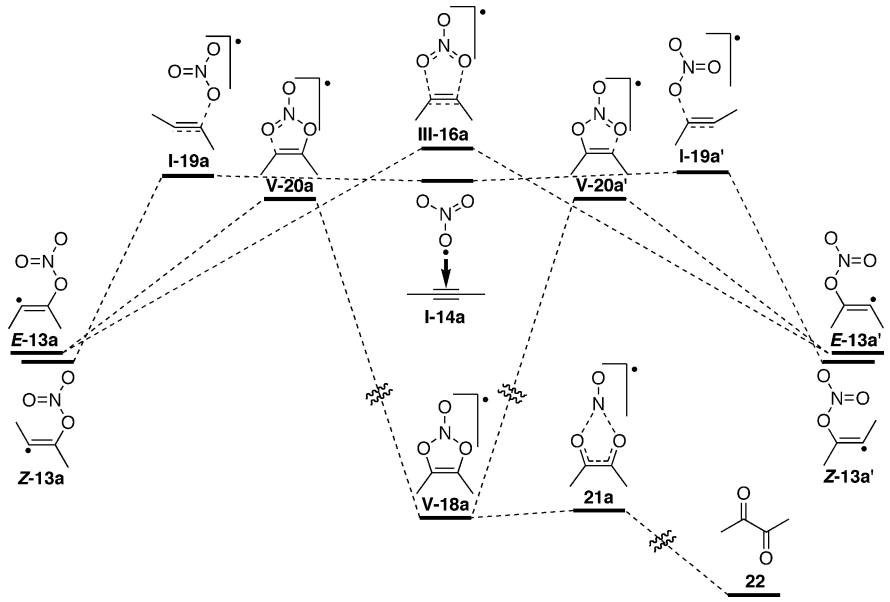

drawn from the ROMP2 single-point computations. Compared with the QCISD and CCSD(T) single-point calculations, ROMP2 overestimates the energies of the association complex **I-14a** and transition state **III-16a**, but calculates energies that are too low for the cyclic intermediate **V-18a**. It was, however, gratifying to see that energies resulting from the computationally very cost-intensive CCSD(T)/cc-pVTZ single-point calculations were very close to those obtained with QCISD and CCSD(T) with the smaller cc-pVDZ basis set.[17] With the exemptions mentioned above, all methods resulted in very similar geometries for all ground and transition states. On average, the best agreement with the QCISD and CCSD(T) single-point computations was found for the calculations at the BHandHLYP/cc-pVDZ level of theory, so that only these data will be discussed here. For additional information, see the Supporting Information.

The lowest energy pathway for the rearrangement of **13a** into **13a′** proceeds out of the *Z*-configurated radical ***Z*-13a** along pathway (I) (see Scheme 2) through reversible fragmentation/radical addition via transition state **I-19a** with formation of an intermediate $NO_3^{\bullet}$−2-butyne association complex **I-14a** (Scheme 3).[18]

The computations revealed an activation barrier of about 90 kJ mol^{-1} or about 82 kJ mol^{-1}, respectively, if the zero-point energy correction (ZPE) is included. The C−O distance in **I-19a** is 2.127 Å with the released/attacking nitrate moiety being twisted out of the plane ($\theta_{NOC^1C^2} = 103.7°$). Spin density can be found on the vinyl carbon (41%) and on two O-atoms of the nitrate moiety, where the attacking oxygen carries 53% (see Figure 1). In the association complex **I-14a**, which is some 3 kJ mol^{-1} lower in energy than **I-19a**, $NO_3^{\bullet}$ is located about 2.5 Å above the alkyne triple bond.

The data would, however, suggest that a rearrangement out of ***E*-13a** along a stepwise ring-closure−ring-opening sequence [pathway (V)] through the cyclic radical intermediate **V-18a** should be more favorable than the above-mentioned fragmentation/radical-addition pathway, because transition state **V-20a** can be reached with an activation energy that is lower by about 15 kJ mol^{-1} (or ca. 11 kJ mol^{-1} with ZPE included) compared to that of **I-19a**. Interestingly, **V-18a** is significantly more stable than its open-chain counterparts, ***E*/*Z*-13a**, by some 120 kJ mol^{-1}. However, the reverse ring opening that would lead to the rearranged radical ***E*-13a′** is not only highly endothermic, but with an activation barrier of about 190 kJ mol^{-1} it is also kinetically unfavorable. **V-18a**, in which the spin density is distributed over the entire nitrate moiety with the majority being located on nitrogen (46%) and on the exocyclic O-atom, O^e (30%; see Figure 1), escapes from this trap through fragmentation into diacetyl (**22**) and nitric oxide, NO$^{\bullet}$, via transition state **21a**. This process requires only about 5 kJ mol^{-1} activation energy and is highly exothermic (ΔE ca. 300 kJ mol^{-1}, determined at the BHandHLYP/cc-pVDZ level of theory).[19] A discussion of the impact of this cyclization/fragmentation pathway on self-terminating radical oxygenations (see Scheme 1) will be given below.

A rearrangement of ***E*-13a** through the symmetrical, planar, five-membered transition state **III-16a** would require about 15 kJ mol^{-1} more energy than the fragmentation/radical-addition pathway via **I-19a**. The C−O distance in **III-16a** is with 2.022 Å slightly shorter than in **I-19a**, and the spin density is nearly equally distributed between the two "ring" O-atoms, which carry 21% each, and the acetylenic carbons, which are carrying 29% each (see Figure 1). A symmetrical or even unsymmetrical three-membered ring transition-state structure of type **II-15a**, which would be formed along pathway (II) (see Scheme 2), could not be located.

Rearrangement of the β-(Acetoxy)vinyl Radical 13b: The geometries of the stationary points in the rearrangement of the

(17) In contrast to the UHF and DFT computations, all single-point calculations revealed a slightly more stable transition state **21a**, compared to that of the cyclic intermediate **V-18a**. Because the pathway involving **21a** is of very minor importance for the current investigation, the reason for this discrepancy was not explored.

(18) IRC calculations have shown that these radical additions to alkynes lead to the *Z* configurated vinyl radical: Wille, U.; Dreessen, T. *J. Phys. Chem. A* **2006**, *110*, 2195.

(19) Interestingly, the UHF calculations revealed a stepwise fragmentation process of **V-18a** into **22** and NO$^{\bullet}$ with two consecutive O−N bond cleavages requiring about 37 and 20 kJ mol^{-1} activation energy, respectively.

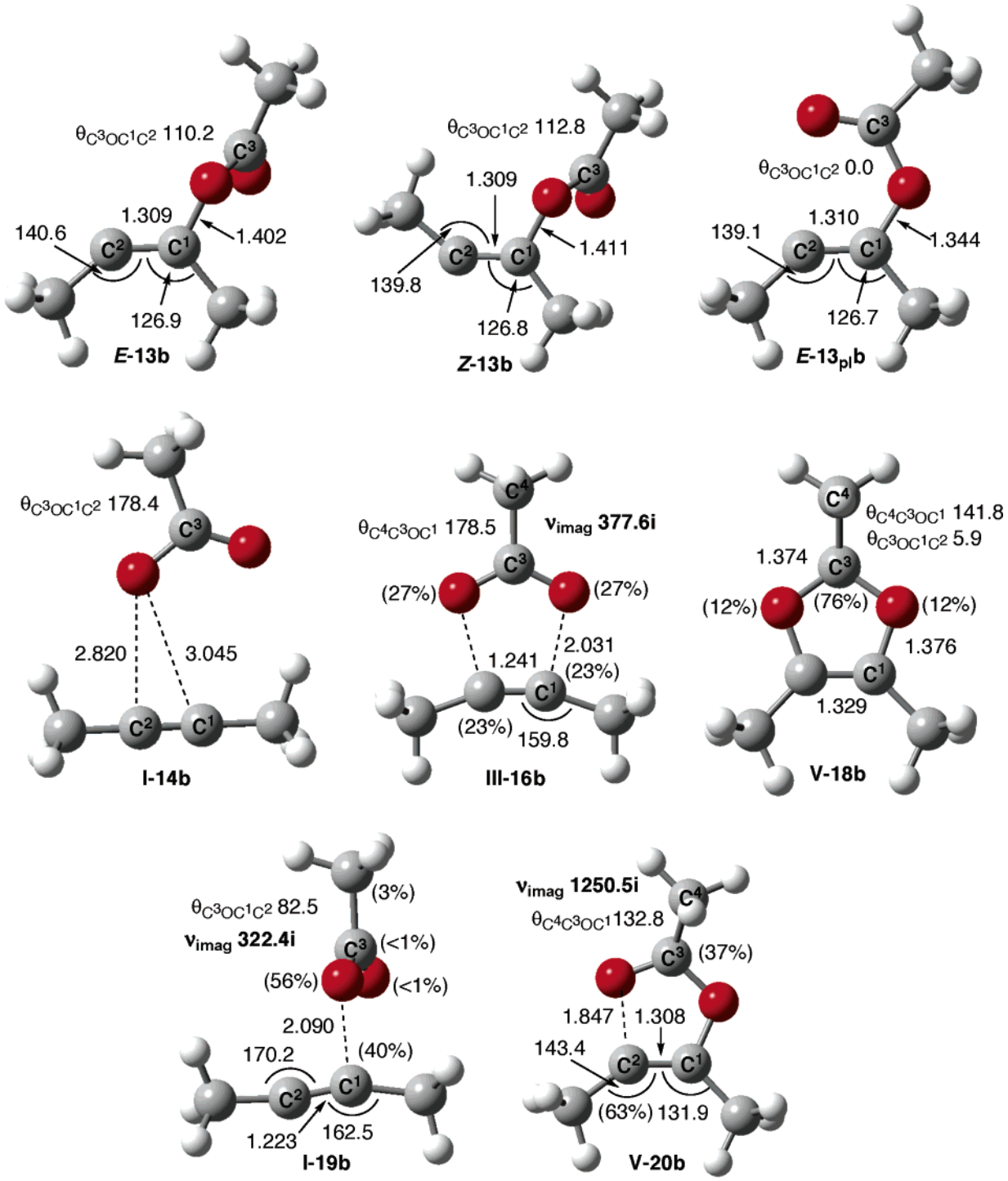

FIGURE 2. Geometrical parameters (bond lengths in Å; angles and dihedral angles, θ, in degrees) of ground and transition states (imaginary frequencies, ν_{imag}, in cm^{-1}) and spin density distributions (in percent, in brackets) for some key structures in the rearrangement of 2-(acetoxy)-2-butenyl radical **13b** (geometries, BHandHLYP/cc-pVDZ; spin densities, BHandHLYP/aug-cc-pVTZ).

β-(acetoxy)vinyl radical **13b** calculated at the BHandHLYP/cc-pVDZ level of theory are shown in Figure 2 and are generally very similar to those found for **13a**, except that (i) also a planar vinyl radical, ***E*-13$_{pl}$b**, was located, which is only insignificantly more stable than ***E*-13b** and that (ii) a transition-state analogue to **21a** leading to the diketone **22** was not found.

The energies are listed in Table 2 relative to ***E*-13b**. Also for this reaction, the results from the BHandHLYP/cc-pVDZ calculations showed a generally satisfactory agreement with the QCISD and CCSD(T) single-point calculations so that only these data will be discussed here. Additional information can be found in the Supporting Information. The potential energy surface for the **13b** → **13b′** rearrangement is shown in Scheme 4.

The cyclic radical intermediate **V-18b**, although lower in energy by about 28 kJ mol^{-1} compared to ***E*-13$_{pl}$b**, is far less stabilized than its nitrate-containing counterpart **V-18a**. The spin density in **V-18b** is distributed between the acyl C-atom (76%) and the two O-atoms (12% each; see Figure 2). A rearrangement

TABLE 2. Relative Energies ΔE (in kJ mol^{-1}) for Stationary Points in the Acyloxyl Shift of 2-(Acetoxy)-2-butenyl Radical (13b)[a]

	E-13b	*Z*-13b	*E*-13$_{pl}$b	I-14b	III-16b	V-18b	I-19b	V-20b
BHandHLYP/	0.0	−3.1	−0.7	83.9	103.5	−22.9	98.1	124.3
6-311G**		*−3.1*	*−1.3*	*73.4*	*97.6*	*−16.6*	*89.0*	*119.5*
BHandHLYP/	0.0	−3.3	−2.2	91.6	108.0	−30.1	105.5	119.1
cc-pVDZ		*−3.2*	*−2.7*	*81.3*	*102.1*	*−23.8*	*96.1*	*114.2*
BHandHLYP/	0.0	−2.0	−0.4	86.8	105.9	−26.7	99.9	123.1
cc-pVTZ		*−2.1*	*0.0*	*75.9*	*100.1*	*−20.2*	*90.7*	*118.4*
BHandHLYP/	0.0	−1.5	−1.0	88.0	105.4	−27.9	99.4	122.6
aug-cc-pVTZ		*−1.5*	*−0.6*	*77.2*	*99.7*	*−21.1*	*90.1*	*118.0*
QCISD/ cc-pVDZ[b]	0.0	−3.8	−0.3	91.9	104.3	−19.9	109.7	116.7
CCSD(T)/ cc-pVDZ[b]	0.0	−3.9	−1.1	95.6	92.8	−22.1	103.9	104.3

[a] Data in italics include the zero-point vibrational energy correction (ZPE). [b] Single-point calculation on BHandHLYP/aug-cc-pVTZ optimized geometry.

SCHEME 4. Potential Energy Surface of the Rearrangement of Radical 13b (BHandHLYP/cc-pVDZ Level of Theory, ZPE Included)

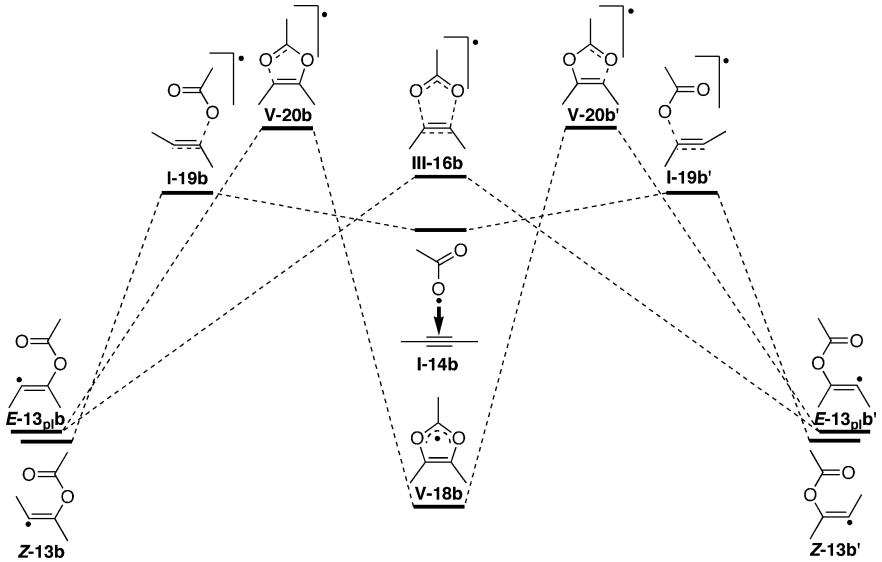

of ***E*-13$_{pl}$b** along pathway (V) (see Scheme 2) via **V-18b** through transition state **V-20b** would require the highest activation energy of all thinkable processes (activation barrier for cyclization ***E*-13$_{pl}$b → V-20b**, about 122 kJ mol^{-1}; activation barrier for ring opening **V-18b → V-20b′**, about 150 kJ mol^{-1}; without ZPE). In contrast to **13a**, the reversible fragmentation/radical addition process out of ***Z*-13b** along pathway (I), via transition state **I-19b** and an intermediate acetoxyl-2-butyne association complex **I-14b**, is energetically practically identical to a rearrangement (out of ***E*-13$_{pl}$b**) through the planar five-membered ring transition state **III-16b** along pathway (III). The fragmentation/radical-addition mechanism requires an activation energy of some 109 kJ mol^{-1} (or ca. 99 kJ mol^{-1}, if ZPE is included), whereas the barrier height for **III-16b** is about 110 kJ mol^{-1} (or ca. 100 kJ mol^{-1} with included ZPE). According to the QCISD and CCSD(T) single-point computations, however, rearrangement through **III-16b** should be even slightly more favorable. The acetoxy group in **I-19b** is arranged nearly perpendicular to the plane of the carbon framework. Spin density can be found mostly on the vinyl C-atom (40%) and the attacking O-atom (56%) and to a very minor extent at the acetyl methyl group (4%). The spin density in **III-16b** is located similar to that in **III-16a**, for example, on both O-atoms (23% each) and both acetylenic carbons (27% each; see Figure 2). In the association complex, **I-14b**, the acetoxy group is arranged coplanar, but slightly unsymmetrical with regard to the carbon chain, as indicated by the C−O distances of 2.820 and 3.045 Å, respectively.

Neither a symmetrical or an unsymmetrical three-membered ring transtion state of type **II-15b**, which could be formed along pathway (II), could be located.

Role of Charge Separation in the Transition States: In the absence of kinetic data, an investigation of charge separation in the transition states of the rearrangement could indicate whether polar solvents may be influencing the mechanism. This could be of significance especially in the case of the acyloxy-vinyl radical **13b**, where rearrangement through the five-membered ring transition state **III-16b** or via reversible fragmentation/radical addition through transition structure **I-19b** requires similar activation energies. Charge separation, which may lead to a contact ion pair [pathway (IV), generalized as structure **IV-17** in Scheme 2], can be characterized through the overall partial charge of the nitroxy or acetoxy fragment in the ground state **13a/b**, compared to that in the relevant transition states **III-16a/b** and **I-19a/b**. The analysis is based on charges from a Mulliken population analysis and a natural population analysis (NPA) computed at the BHandHLYP/aug-cc-pVTZ level of theory, to take also the influence of the various lone pairs into account. The respective group charges have been

TABLE 3. Nitrate and Carboxylate Group Charges in Ground and Transition States for the Rearrangement of 13a and 13b (BHandHLYP/aug-cc-pVTZ)

	13	III-16	I-19
	a: Y = N, Z = O		
Mulliken	−0.563	−0.716	−0.516
NPA	−0.345	−0.544	−0.401
	b: Y = C, Z = Me		
Mulliken	−0.509	−0.585	−0.442
NPA	−0.320	−0.446	−0.358

obtained as the sum over the partial charges of the contributing atomic centers (Table 3).

The group charges obtained from the Mulliken analysis are generally higher than those from the NPA. In the fragmentation/radical-addition transition states, **I-19a/b**, the Mulliken charges are slightly decreasing by about 10%, compared to the vinyl radicals **13a/b**, whereas the NPA shows an increase of about 18% for both nitrate and carboxylate group. In contrast to this, the increase in charge by 27% (Mulliken) and 58% (NPA), compared to the nitroxyvinyl radical **13a**, indicates a significant charge separation in the five-membered transition state **III-16a**. In the case of the carboxylate group in **III-16b**, the charge increase is with 15% (Mulliken) and 39% (NPA), compared to that of **13b**, which is somewhat smaller but still obvious. In both cases, the amount of charge separation may be not large enough to classify transition state **III-16a/b** as a contact ion pair **IV-17a/b**, but at least a serious amount of polarization is apparent. From this it may be concluded that polar solvents should have a larger impact on the barrier height of **III-16a/b** than on **I-19a/b**.[20] Thus, whereas for the rearrangement of **13b** in the gas-phase transition states **I-19b** and **III-16b** are competing, it is very much possible that the group migration proceeds exclusively via **III-16b** in solution. On the other hand, the influence of solvation on the rearrangement rate and mechanism in the case of **13a** cannot be predicted. The fragmentation/radical-addition pathway via transition state **I-19a** is energetically favored by about 20 kJ mol^{-1} over the cyclic five-membered transition state **III-16a**, and whether solvation effects can overcompensate this difference is difficult to say. [21]

Comparison of the Experimental Data with the Calculated Rearrangement Pathways of 13a and 13b: On an absolute scale, the calculated reaction barriers appear to be too high to be important for short-lived radical intermediates. This discrepancy could be due to the fact that the calculations were performed for the gas phase, where the rearrangement might be slower than in solution.[20] However, an inspection of the data in Tables 1 and 2 reveals that all computational methods used in this work show essentially the same trend for the energies of the various ground and transition states. The following discussion will therefore focus on the relative energy differences between the different pathways.

According to the calculations, the 1,2-rearrangement in the nitroxyvinyl radical **13a** through reversible fragmentation/radical addition via transition state **I-19a** is energetically favored by about 20 kJ mol^{-1}, compared to the same process in the acyloxyvinyl radical **13b**. However, the experiments would suggest a faster rearrangement in an acyloxyvinyl radical **2** or **3** [with X = RC(O)], than in a nitroxyvinyl radical (with X = NO_2), to explain the high yields of the spiro diketone **10** in the reaction of acyloxyl radicals with **1** (see Scheme 1).

SCHEME 5

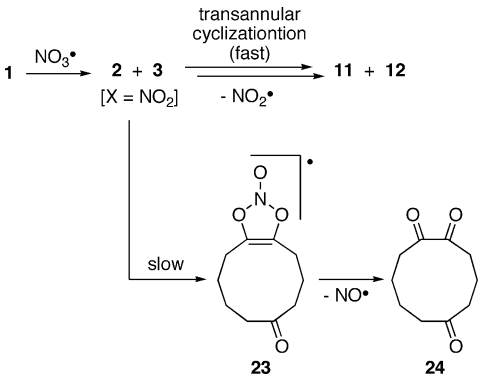

This apparent discrepancy between the experimental results and the computational predictions could be untangled by suggesting that the radical cyclization/homolytic fragmentation process **2/3 → 5/6 → 8/9 → 11/12** is fast and irreversible if X = NO_2, but not when X = RC(O). To explore this possibility, the activation barrier for the homolytic scission of the O−NO_2 bond in radicals of type **8/9** was calculated for a simplified model system at the BHandHLYP/cc-pVDZ level of theory and found to be only 2 kJ mol^{-1}. Thus, when X = NO_2, the generally fast reverse ring opening of an oxiranyl radical,[22] for example **8/9 → 5/6**, cannot compete with the terminating, very exothermic fragmentation step.[23] It may, therefore, be concluded that once the vinyl radicals **2/3** (with X = NO_2) are formed, they proceed directly to the products **11** and **12**, and there is no time for a 1,2-rearrangement of the nitroxyl moiety in the vinyl radicals. On the other hand, the final homolytic scission of the C−O bond in an acetoxy group was calculated to require some 133 kJ mol^{-1} (BHandHLYP/cc-pVDZ), and it is not unlikely that this step is even rate-determining. Thus, with X = RC(O), the reverse reactions of the entire cyclization sequence, including the 1,2-rearrangement in the vinyl radicals **2/3**, either via the fragmentation/radical-addition pathway (I) or via a five-membered cyclic transition state (III), are becoming important, and the ratio of the products **10**−**12** reflects the competition between the various different reaction pathways.

Impact of the Fragmentation Process III-18a → 22 on "Self-Terminating Radical Oxygenations": The activation barrier for the cyclization of nitroxyvinyl radical **13a** to the five-membered ring intermediate **III-18a** was found to be below that of the fragmentation/radical-addition process. Because **III-18a** can undergo a fast fragmentation into diacetyl **22** and NO•, formation of 1,2-diketones should generally be a major pathway in the reaction of NO_3• with C≡C triple bonds.

The finding that a triketone **24** is not produced in the reaction of NO_3• with cycloalkynone **1** (Scheme 5) leads to the conclusion that the transannular 5-exo or 6-exo radical cyclization, respectively, of the vinyl radicals to the transannularly

(20) Solvent effects were not included in the present investigation. The theoretical treatment of solvation is accompanied with many assumptions and simplifications so that in the absence of experimental data the quality of the results is difficult to judge.

(21) Significant solvent effects with a barrier reduction of some 20 kJ mol^{-1} have been measured for saturated counterparts of **13b**, for example, *β*-(acetoxy)ethyl radicals, on moving from *tert*-butylbenzene to water as reaction medium; see ref 8b.

(22) (a) Laurie, D.; Nonhebel, D. C.; Suckling, C. J.; Walton, J. C. *Tetrahedron* **1993**, *49*, 5869. (b) Krishnamurthy, V.; Rawal, V. H. *J. Org. Chem.* **1997**, *62*, 1572.

(23) Wille, U.; Dreessen, T. Unpublished results.

activated carbonyl group (**2/3** → **5/6**) must be faster than cyclization to a five-membered radical intermediate of type **23**. However, 1,2-diketones are indeed formed as byproducts or even major products in reactions of $NO_3^\bullet$ with certain open-chain alkynes.[2b,24]

Conclusions

Computational studies have revealed that the 1,2-nitroxyl rearrangement in β-(nitroxy)vinyl radical **13a** should proceed through a reversible fragmentation/radical-addition pathway via transition state **I-19a** and an intermediate $NO_3^\bullet$−2-butyne association complex **I-14a**. Rearrangement through a five-membered ring transition state **III-16a** is clearly disfavored by about 20 kJ mol^{-1}. In contrast to this, in the β-(acetoxy)vinyl radical **13b**, the fragmentation/radical-addition pathway via transition state **I-19b** and a rearrangement through the five-membered ring transition state **III-16b** are competing processes. The rearrangement of **13b**, however, requires some 20 kJ mol^{-1} more activation energy than the group migration in **13a**. Mulliken and NPA revealed a modest amount of charge separation in the transition states **I-19a/b**. In contrast to this, the charge separation in transition states **III-16a/b** was found to be not insignificant, which may indicate a potential solvent effect on the rearrangement rate and mechanism, especially for **13b**. For both **13a** and **13b**, a pathway involving a cyclic three-membered ring transition state of type **II-15** was not found.

A rearrangement through a cyclic radical intermediate **V-18a/b** can also be ruled out for both vinyl radicals, but for different reasons. Cyclization of the acyloxyvinyl radical **13b** to **V-18b** via transition state **V-20b** is kinetically the least favorable of all processes studied for this vinyl radical. In contrast to this, cyclization to **V-18a** is kinetically and thermodynamically the most favorable process for the nitroxyvinyl radical **13a**, but it is irreversible because the activation barrier for the reverse ring-opening of **V-18a** to the rearranged radical **13a′** is about 190 kJ mol^{-1}, which is extremely high. **V-18a** escapes from this trap by unimolecular fragmentation into NO$^\bullet$ and the 1,2-diketone **22**. The experimental result that 1,2-diketones are not produced in the reaction of $NO_3^\bullet$ with the cycloalkynone **1**, although such a fragmentation pathway should be highly favorable according to the calculations, shows that transannular radical cyclizations in the vinyl radicals **2/3** are even faster than a cyclization to a five-membered radical intermediate **23**.

The calculations lead to the conclusion that, in the case of the $NO_3^\bullet$-induced radical oxygenation of cycloalkyne **1**, all processes following the initial $NO_3^\bullet$ addition to the C≡C triple bond are fast and irreversible, because the terminating homolytic scission of the O−N bond requires practically no activation energy. Thus, a 1,2-rearrangement of the nitrate moiety in a vinyl radical has no time to occur. In contrast to this, it is likely that in radical oxygenations involving acetoxyl (and other O-centered radicals, see Scheme 1), the final homolytic cleavage of the O−C bond is the rate-determining step. In these systems, all cyclization steps are not only reversible, but there is also enough time for a 1,2-rearrangement of the acetoxy group in the vinyl radicals. The ratio of the products **10**−**12** reflects, therefore, the relative rates between the various competing processes.

The calculations showed a significant method-dependent outcome. Both, the very popular B3LYP method as well as mPW1PW91 and MP2 failed to locate important geometries on the potential surface of the rearrangement of **13a**, and neither DFT method used in this work could locate the planar nitroxyvinyl radical ***E*-13$_{pl}$a**. Despite this, both the mPW1K and the BHandHLYP methods could locate all relevant ground and transition states in the rearrangement process. Although the calculated geometries are largely similar at the various levels of theory, a comparison of the computed energies with single-point calculations performed at correlated levels showed the best agreement with the BHandHLYP/cc-pVDZ level of theory. In contrast to this, the computed energies using the UHF and MP2 method were significantly too high. This shows that a careful assessment and benchmarking of the computational outcomes is essential for the theoretical investigation of these reactions. Future experimental and computational studies will reveal the influence of solvents on the mechanism of the radical rearrangement and cyclization shown in Scheme 1.

Acknowledgment. This work was supported by the Australian Research Council under the ARC Centres of Excellence program and the Victorian Institute for Chemical Sciences High Performance Computing Facility, and the Australian Partnership for Advanced Computing. I thank Professor Carl H. Schiesser, The University of Melbourne, for helpful discussions, and Dr Tim Dreessen for his support.

Supporting Information Available: Gaussian output files for all structures. This material is available free of charge via the Internet at http://pubs.acs.org.

JO0520543

(24) Andropof, J.; Wille, U. Unpublished results.